NME_2016_213

Deuterium retention in MeV self-implanted tungsten: influence of damaging dose rate

T. Schwarz-Selinger

Max-Planck-Institut für Plasmaphysik, Boltzmannstr. 2, D-85748 Garching, Germany

E-mail: schwarz-selinger@ipp.mpg.de

Abstract.

Recrystallized, polycrystalline tungsten was self-damaged by 20 MeV tungsten ions up to a calculated damage dose in the damage peak of 0.23 dpa. The time to acquire this dose and hence the average damaging dose rate was varied from 6×10^{-3} to 4×10^{-6} dpa/s, the latter coming close to the damage dose rate expected from fusion neutrons in future devices such as ITER and DEMO. One series was conducted at 295 K and one at 800 K to check for possible effects of defect evolution at elevated temperature. The created damage was decorated afterwards with a deuterium plasma at low ion energy of < 15 eV and low flux of 5.6×10^{19} D/m^2 until saturation to derive a measure for the defect density that can retain hydrogen isotopes. ^{3}He nuclear reaction analysis (NRA) was applied to derive the deuterium depth profile and the maximum concentration in the damage peak. Neither for the 295 K nor for the 800 K series a variation in deuterium retention with damage dose rate was found.

Keywords: tungsten, deuterium retention, displacement damage, plasma, NRA, Plasma-material interactions, ion radiation effects

1. Introduction

Taking co-deposition with low-Z elements aside hydrogen isotopes retention in present-day fusion devices with tungsten walls is limited by intrinsic and near-surface, plasma-induced defects. In contrast, in a future thermonuclear fusion device additional trapping sites will be created throughout the tungsten bulk by fast fusion neutrons which will potentially increase retention by orders of magnitude. Recent experiments with fission-neutron-irradiated tungsten show after deuterium plasma exposure deuterium concentrations of up to 0.8 at.% at 200°C [1]. However, these studies are hampered by the fact that neutron exposure conditions are not well defined in terms of temperature and dose rate. In addition handling and analysis of these activated samples are typically very limited, turn-around times are long, experiments are expensive, and because of that samples are typically few. Systematic parameter studies are therefore not available. To overcome these limitations, ions with energies of tens of keV to MeV are often used as surrogates to create displacement damage. They are successfully applied since decades in fission material development for lifetime tests such as swelling [2]. For fuel retention studies in tungsten, high energy ion implantation is used since many years and it is still a field of active research [3, 4, 5, 6, 7]. Contrary to neutron irradiation, ion-beam irradiation is fast and does not activate the samples. However, it is still unclear in how far the observations gained with this ion-beam-damaged surrogate material can be transferred to material damaged with fusion neutrons. Different ions and different energies are used and it is not clear in which case the displacement damage resembles best the defect structure created by the collision cascades with fast fusion neutrons. One

parameter that was not addressed yet is the vast difference in the damage creation rate between ion-beam damaging and damage created by fusion neutrons. There is some doubt that the biggest advantage of high energy ion implantation, namely its accelerated speed, might create artefacts that would not be present if damage creation would be conducted at the rate expected in the future fusion application. While for the latter damage doses in the dpa range are acquired over a year they can be collected within hours with an ion beam or even faster and hence damaging dose rates for ion-beam damaging are typically at least two to three orders of magnitude larger than expected for future fusion devices. A prominent example for a rate-dependent effect in ion-beam irradiation of materials is the peak swelling temperature in steels that was found to be higher for higher dose rates in simple metals such as copper, nickel or stainless steel [2]. Because of this rate dependence of such swelling experiments it was also concluded that it is not advisable to scan the ion beam with high frequency over the sample when trying to simulate neutron damage [2]. Nevertheless it is applied in most studies on D retention in order to achieve a homogenous implantation profile as it facilitates later analysis. Unfortunately such essential experimental details are very often not even mentioned explicitly in the literature which hampers the comparability of results even between these surrogate studies. In this contribution the experimental setup for MeV ion implantation used over the last years at IPP Garching is first explained in detail. Second, results on deuterium retention for tungsten implantation into tungsten – so-called self damaging – will be presented. Special emphasis is placed on the influence of the damaging dose rate on retention. Damaging with continuous and scanned ion beam will be compared.

2. . Experiment

Hot-rolled tungsten with a purity of 99.97 wt.%. manufactured by Plansee AG (Austria) [8] was used in this study. In order to assure comparability and to minimize the influence of micro-structural effects all W samples were from the same manufacturing batch as in preceding studies [6, 7, 9, 10, 11, 12] 13, 14, 15]. For this study the sample size was 10×10×0.8 mm^3. The main impurity, excluding Mo, in this W grade is carbon and iron with less than 30 µg/g each. To allow for reliable determination of depth profiles with ion-beam methods the surfaces were chemo-mechanically polished to a mirror-like finish following the procedure outlined in reference [10].

The aim of this study was to focus on the defects created by the self-damaging. Therefore, intrinsic defects as well as possible gaseous inclusions were minimized by re-crystallizing the specimen in vacuum. First, samples were carefully outgassed and finally heated to 2000 K for 2 min by electron bombardment while maintaining the pressure in the low 10^{-6} Pa range. The temperature was measured with a disappearing filament pyrometer during this procedure. As a consequence of this re-crystallization, the initial dislocation density of 2×10^{12} m/m^3 is reduced by two orders of magnitude compared to the as-delivered state [11]. The material exhibits grains with a size distribution ranging from 10 µm to 50 µm as observed by scanning electron microscopy and by confocal scanning laser microscopy. An image of a representative surface area of 100 µm by 133 µm is shown in figure 1. Because recrystallization is performed after polishing, distortions introduced by the polishing procedure are annealed out, too.

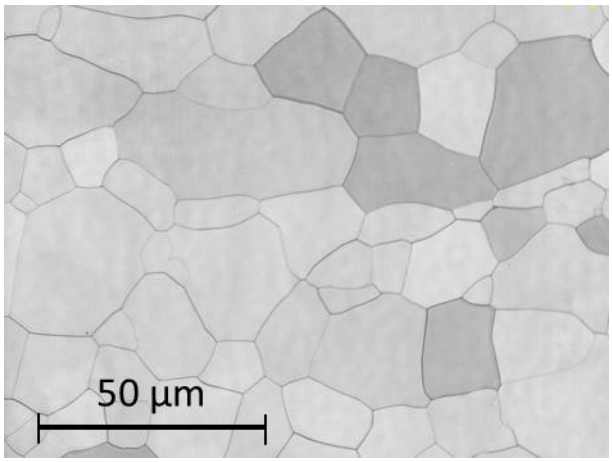

Figure 1: Confocal laser scanning microscopy image of a sample surface after polishing and annealing at 2000 K for 2 min in UHV.

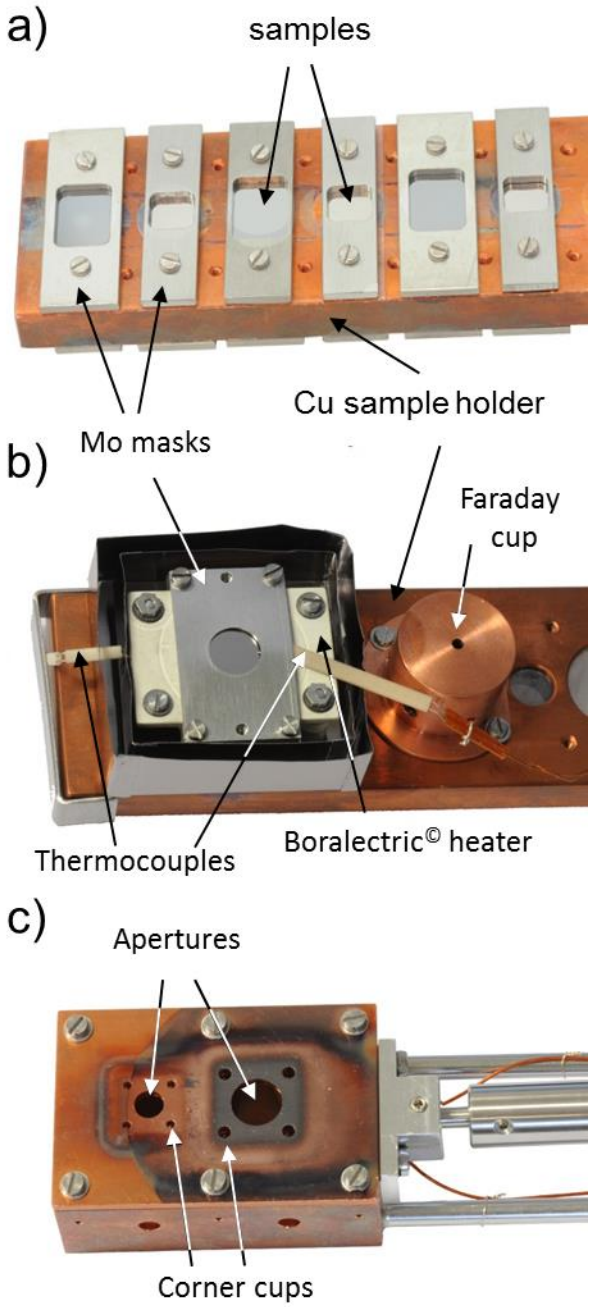

Figure 2: Sample holders for MeV tungsten implantation used in this study. a) water-cooled holder with 10x10 mm^2 samples and 12x15mm^2 reference samples clamped down with molybdenum masks. b) holder for implantation at elevated temperature showing the Boralectric© heating element, the two thermocouples, the Mo radiation shields, a sample installed with the molybdenum mask and the faraday cup for beam characterization. c) beam-defining, water-cooled apertures 7 mm and 12 mm in diameter together with the four corner cups for in situ current measurement.

93

Damaging was done by tungsten self-implantation with 20 MeV W^{6+} ions in the TOF beamline of the 3 MV tandetron accelerator. Tungsten ions were created with a cesium sputter source from a tungsten carbide target. For the first experimental series samples were directly clamped down with a molybdenum mask on a water-cooled copper substrate holder as shown in figure 2a. The mask opening area was 9 x 9 mm^2 in this case. For the second series at elevated temperature, samples were mounted directly on a resistive heater (Boralectric© HTR1001) and also clamped down with a molybdenum mask as shown in figure 2b. A rectangular mask with a circular opening of 9 mm in diameter was used in this case. In the present high-temperature design two thermocouples are used to allow for reliable temperature control of the sample. One type K thermocouple was inserted into a small hole at the side of the heater itself, a second type K thermocouple was clamped between the sample and the mask as shown in figure 2b. To minimize outgassing and to achieve a quick response time to temperature changes the heater is mounted on a water-cooled support structure and surrounded by molybdenum shields as can be seen in figure 2b, too. Typically the W beam is focused onto the target position with an electrostatic quadrupole triplet lens and scanned over an area of up to 25 mm by 25 mm to achieve a homogenous flux throughout the implantation area. For the latter x- and y-deflection plates are used whose voltage supply is ramped with two triangle wave-shaped crystal-locked scan frequencies of close to 1 kHz. Water-cooled copper apertures with different size are placed in front of the sample holder arrangement that have four faraday cups in the corners and a central hole as shown in figure 2c. When the beam is spread out to cross the four corner cups, the absolute tungsten flux can be calculated from the measured current and the cup surface areas. A central hole in the

copper aperture defines the beam that finally hits the sample. This aperture is aligned with the sample mask using an optical telescope on axis. For this study, arrangements with a central hole of 12 mm and 7 mm in diameter were used. Figure 3 shows experimental results to characterize the beam. To measure its width the beam was focused and steered into one of the four corner cups with a diameter of 2 mm while manually moving the cup (red circles and left scale). In addition, deuterium retention measured with NRA of a sample implanted with 20 MeV W^{6+} with the focused beam to a fluence of 7.87×10^{17} W/m^2 and subsequently exposed to D plasma at 295 K till saturation is reached. Figure 3 shows integrated proton counts from the D(^{3}He,p)α nuclear reaction measured with a ^{3}He energy of 2.4 MeV while scanning laterally over the sample (blue stars and the right scale). The analyzing spot width was 1 mm in that case. Both experiments show the same beam width at half maximum of 2 mm.

Also shown in Figure 3 are the integrated proton counts of a sample implanted with the beam spread out to homogenize the implantation (open blue squares). The sample was also exposed to D plasma to decorate the defects until saturation at 295 K and measured with a ^{3}He energy of 2.4 MeV while scanning laterally over the sample. The observed variation in D retention of 2 % is within the accuracy of the NRA analysis. We hence conclude a homogeneity of the W implantation of better than 2 %.

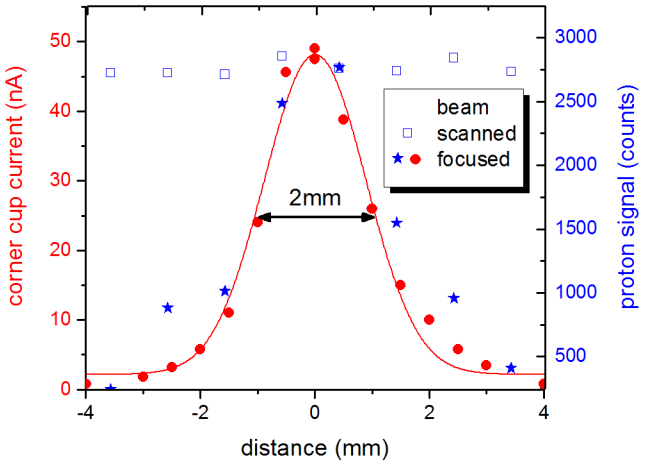

Figure 3: Beam-profile measurement of the focused W beam. Red circles and left scale show the current measured in one of the four corner cups while manually moving the cup. In blue and the right scale integrated proton counts from the D(^{3}He,p)α reaction are shown from a scan laterally over the sample implanted with the focused beam (blue stars) and the scanned W beam (open squares). ^{3}He energy 2.4 MeV. In addition a Gaussian curve is plotted to guide the eye.

The current measurement from which the average W flux and hence the total fluence is deduced was cross checked with implanting W^{2+} with an energy of 1 MeV and a fluence of 1.6×10^{20} W/cm^2 into mirror-polished pyrolytic graphite and subsequent Rutherford Backscattering Spectrometry of the implanted tungsten amount with 1 MeV protons. Comparison of the measured spectra with SIMNRA 6.06 [16] simulation yields an accuracy better than 10% for the absolute amount of tungsten and hence for the W ion current measurement.

The measure for the damage dose is derived in this work by evaluating the computed displacements from SRIM-2008.04 calculations [17]. Care must be taken when comparing this quantitatively to values stated in the literature. Besides obvious differences when using different displacement energies (e.g. 68 eV in [5], or 90 eV in [18] subtle changes can exist using different releases of the code as well as different calculation volume or number of ions. Much more seriously, with the very same

parameters but different calculation options (“Quick Kinchin Pease” or “Full Cascade”) or evaluating different output files (vacancy.txt or e2recoils.txt) there might be a difference up to a factor of two depending on the procedure applied as stressed by Stoller et al. and Nordlund et al. [19, 20]. These two studies recommend using the “Quick Kinchin Pease” option and it is hence used in this study. Unfortunately, most of the work to be found for self-damage tungsten in literature till now applied the “Full cascade” option, but in none of them the necessary input parameters and procedures applied are given. In this study “dpa” values are calculated using SRIM-2008.04 adding the “recoil” and “ion” displacements from the “vacancy.txt” output file and converting the sum with the ion fluence and the tungsten density to get a depth profile of the number of displaced target atoms and the damage dose in “displacements per atom”, in short “dpa”. Replacement collisions are neglected. A displacement energy of 90 eV as recommended by the American Society for Testing and Materials [21] is used and a lattice binding energy of 0 eV. The results of the here applied “Quick Kinchin Pease” calculation option are compared with those of the “Full Cascade” calculation option to allow easy comparison with existing values in literature. For the here investigated case of 20 MeV tungsten self-implantation the “vacancy.txt” output yields for the “Quick Kinchin Pease” calculation 1.86 displacements per ion and Ångström in the peak maximum while it is 4.05 displacements per ion and Ångström for the “Full cascade” option and hence a factor of 2.2 less. It is important to note here that this factor is not unique, but varies with energy.

Loading of the samples with deuterium was performed in the well-characterized low-temperature plasma experiment PlaQ [22]. To decorate only the existing defects with

171 deuterium without creating additional trapping sites, deuterium exposure was performed
172 with floating target holder. At a D_2 background pressure of 1.0 Pa this results in an ion
173 energy below 15 eV. Because the ion flux consists mainly of D_3^+ ions (94 %) with minor
174 contributions of D_2^+ (3 %) and D^+ (3 %) [22] I refer to this setting as <5 eV/D. For this
175 condition the resulting deuterium flux in the form of ions is 6×10^{19} D/m^{2}s. The flux of
176 neutral atomic deuterium of low energy (< eV) exceeds the flux of ions by at least one
177 order of magnitude [22]. However, contributions of neutral atomic deuterium are
178 neglected here and flux refers here to the ion flux only. All samples of one damage-rate
179 series were always D loaded at the same time. Each sample was tightly screwed at the
180 four corners with molybdenum screws to a tungsten-coated copper target holder. To
181 avoid any defect annealing or defect evolution a sample temperature of 295 K was set
182 during D loading. The time was chosen large enough to allow for D diffusion into the
183 depth which is for the given defect density and depth distribution achieved after 72 hours
184 of exposure or a D fluence of 1.5×10^{25} D/m^2. The temperature of the target holder was
185 maintained by a liquid cooling circuit connected to a thermostat operated with ethanol at
186 293 K. Sample temperature was measured with a type K thermocouple spring loaded
187 through a hole in the sample holder touching the back side of one sample. In addition, an
188 IR camera was used to monitor the temperature evolution as well as the lateral
189 homogeneity of all samples during the experiments.

190 Deuterium depth profiles were analysed ex-situ with the D(^{3}He,p)α nuclear
191 reaction with eight different ^{3}He energies varying from 500 keV to 4.5 MeV to probe a
192 sample depth of up to 7.4 µm. The D concentration within the near-surface layer at
193 depths of up to about 0.3 µm was determined with ^{3}He energies of 500 keV, 690 keV and

194 800 keV by analyzing the emitted α particles with a surface barrier detector at the
195 laboratory scattering angle of 102°. A rectangular slit in front of the detector reduces the
196 solid angle to 8 msr but increases resolution. For determining the D concentration at
197 larger depths, the high energy protons were analysed using a thick, large-angle solid state
198 detector at a scattering angle of 135°. A curved slit is installed in front of the detector to
199 increase resolution which reduces the solid angle to 75 msr. A nominal charge of 10 μC
200 was usually accumulated for each energy. Under 165° backscattered ^{3}He was detected
201 with a small surface barrier detector to accurately determine the actually acquired total
202 charge collected for each energy by simulating the spectra with SIMNRA 6.06 [16].
203 NRADC [23] was used for the deconvolution of the spectra measured at different ^{3}He ion
204 energies. As input data for NRADC all α and proton spectra measured at the different
205 energies were analysed simultaneously. Details about the data evaluation using NRADC
206 can be found in Ref. [23]. The present version of NRADC allows to define a depth
207 resolution as a function of depth within the Markov chain sampling. If a layer thickness
208 below that physical limit is proposed this solution is rejected. ResolNRA [24] was
209 applied to define this physical limit. For the quantitative analysis we used the cross
210 section recently published by Wielunska et al. for the protons [25] and Möller and
211 Besenbacher for the α particles [26]. The total amount of D retention up to a depth of
212 7.4 μm was finally determined by integrating the D profile over depth. For energy
213 calibration purposes, to check the performance of the detectors and to calibrate the solid
214 angles of all detectors in-situ amorphous, deuterated carbon thin film samples (*a*-C:D)
215 were measured always together with the samples of interest for each energy. With these
216 precautions the accuracy of the measurement can be reduced to that of the beam-current

measurement which is 3 %. Given the counting statistics (counts depending on D content and energy) the absolute accuracy of the measurements reduces to the absolute accuracy of the cross section which is stated as 5 % [26].

3. Results and discussion

One possible way of changing the implantation flux and hence the damage dose rate would be to use different charges states, because their abundance varies after stripping the primary W^- beam at the terminal of the tandem accelerator. However, for a fixed terminal voltage this leads to different energies of the particles and hence the ambiguity introduced by the different SRIM outputs would make it complicated to compare. Alternatively one could adjust the energy such that the product of charge state and energy stays the same. However, one would reduce the implantation depth to well below half a micron which is impractical as it is then below the depth resolution of the NRA method. Because of the uncertainty in dpa calculations and the limited accessible dynamic range the W implantation energy was kept fixed at 20 MeV in the experimental series presented here, and the tungsten flux was varied instead. By doing this, one can directly compare the experimental results as they are independent from the actual damage profile or the absolute damage dose level.

A previous study for this material grade with 20 MeV self-implantation at room temperature showed that below a damaging fluence of 1.6×10^{16} W/m^2 deuterium retention increases linearly with damage dose, starts to deviate at higher fluences and finally saturates [15]. Above 7.87×10^{17} W/m^2 no further increase in maximum deuterium concentration and deuterium retention with damage dose was observed. This damage saturation regime is selected for this study. Figure 4 shows the respective SRIM

241 calculation converted into damage dose. For the “Full cascade” option a peak damage
242 dose level of 0.5 dpa_{FC} is obtained for this fluence, while it is 0.23 dpa_{KP} for the “Quick
243 Kinchin Pease” option as depicted in figure 4. In addition to the SRIM profile the
244 deuterium depth profile is shown in figure 4. It was derived by deconvoluting the NRA
245 data for a sample self-damaged with the standard conditions comparable to those in
246 previous publications (see [7, 14, 15]) and decorated with D plasma at 295 K. Here, the
247 tungsten beam was spread out to reach the four corner cups to have real time control of
248 the implantation flux. Under these standard conditions one needs an implantation time of
249 43 minutes to reach the intended dose of 7.87×10^{17} W/m^2 and hence the average damage
250 does rate is 8.9×10^{-5} dpa_{KP}/s. It is important to recall here that this value is an average
251 dose rate. The peak dose rate is larger due to the beam scanning with 1 kHz. From the
252 measured beam width shown in figure 2 and the actual scan width the peaking factor can
253 be derived which is in the present experiment a factor of 65 and hence the peak damage
254 dose rate is 5.8×10^{-3} dpa_{KP}/s.

255 Because of the mentioned saturation with damage dose above 0.1 dpa_{KP} the final
256 D depth profile at the here investigated 0.23 dpa_{KP} is not expected to follow the SRIM
257 calculation, but should be rather flat in accordance to the experimental observation. As
258 can be also seen in figure 4 the maximum depth coincides well with the depth predicted
259 by SRIM. The error bars given in the depth profile reflect only the statistical uncertainties
260 determined by NRADC and, thus do not describe the total uncertainty of the
261 measurement mentioned in the previous section. The total amount of deuterium retained
262 in the self-damaged layer is 2.3×10^{21} D/m^2. In the following the maximum deuterium
263 concentration (at the position of the damage peak, i.e. at about 1.3 µm) will be used as it

is easier to compare to implantations at different ion energies, different ions or even to neutron-irradiated material. The maximum deuterium concentration for this experiment is 1.9 at.%.

As stated in the previous section the average implantation flux can be reduced by spreading the beam with the beam sweeping system even further - in the present case by another factor of four compared to the standard condition outlined before. However, by doing so the peaking factor is increased accordingly and hence the peak damage dose rate is not reduced. However, the primary tungsten flux can be reduced by reducing the temperature of the molybdenum thermal ionizer in the sputter source to reduce the primary cesium ion flux. By doing so, the peak damage does rate can be reduced by a factor of five. By applying both, the time to reach 0.23 dpa_{KP} was increased to 16.5 hours in that way. This converts to an average damage dose rate of 3.9×10^{-6} dpa_{KP}/s or a peak rate of 1.3×10^{-3} dpa_{KP}/s. The obtained depth profile is within the accuracy of the method identical to the one shown in figure 4 and the maximum deuterium concentration is 1.8 at.%.

To measure the peak damage dose rate for the standard conditions the beam scanning unit was switched off and the W beam was focused into one of the Faraday cups to measure the W flux. In addition, one target was implanted with this focused beam. By doing this the intended W fluence can be acquired within 40 seconds which converts to a dose rate of 5.8×10^{-3} dpa_{KP}/s in perfect accordance with the value derived from the peaking factor above. Again, the obtained depth profile is within the accuracy of the method identical to the one shown in figure 4. The maximum deuterium concentration in this case is again 1.8 at.%. The maximum concentrations of these three measurements are plotted as

function of average damage dose rate in figure 5a and as function of peak damage rate in figure 5b. It is also worth mentioning that the sample prepared with the continuous beam shows the identical D retention as a sample prepared with a different average damage rate but the same peak damage rate. In summary, variation of the average damage dose rate by three orders of magnitude between 5.8×10^{-3} to 3.9×10^{-6} dpa_{KP}/s or the peak damage rate by a factor of five between 5.8×10^{-3} to 1.3×10^{-5} dpa_{KP}/s does not influence deuterium retention when damaging is conducted at room temperature. Assuming a typical size of a cascade of several tens of nanometer, the given damage creation rate and a typical life time of the primary damage of a few tens of picoseconds [2] this result could have been expected. However, it was not clear from the beginning if longer-time scale effects play a role in damage evolution caused by thermally activated processes. While vacancies are immobile at room temperature due to their large migration barrier of 1.6 eV, tungsten interstitials can migrate (0.05 eV migration barrier) [27]. Although these two defect types are only the easiest to consider and self-damaged tungsten contains many more defect types such as vacancies clusters of different size and dislocations of different geometries their energies are here only used for illustration. Obviously the timescales for defect evolution are shorter as would be required to have any effect on deuterium retention. Likewise defect evolution – such as clustering of vacancies - could take place without influencing deuterium retention.

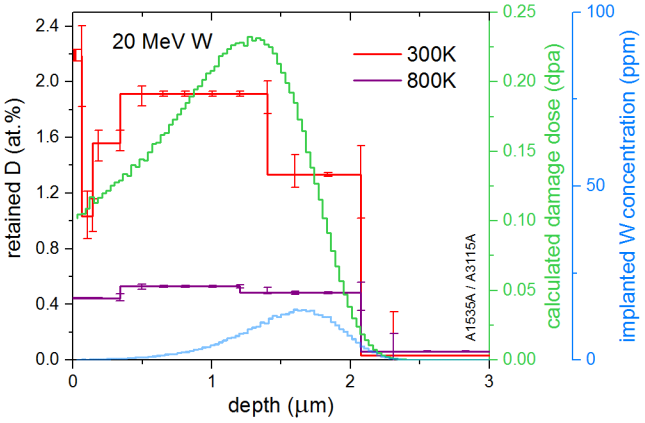

Figure 4: Deuterium depth profile for 20 MeV self-damaged tungsten samples implanted with W^{6+}at 295 K and 800 K with an implantation fluence of 7.87×10^{17} W/m^2 and an average dose rate of 8.9×10^{-5} dpa/s. D decoration was done for 72 h (1.45×10^{25} D/m^2) with <5 eV/D at 295 K. In addition the damage dose (green) and the implanted tungsten concentration (blue) calculated with SRIM 2008.04 as described in the text is shown on the right axis.

According to Keys and Moteff annealing of defects in tungsten sets in at 0.15 times the melting temperature which corresponds to 550 K [28]. Therefore, the experimental sequence was repeated well above that temperature, namely at a damaging temperature of 800 K. Again the average and peak damage dose rate was varied in the same manner as before. Again the depth profile obtained for the sample prepared with "standard" conditions and decorated with D by a deuterium plasma at 295 K is show in figure 4. As expected the depth profile is again flat and reaches to the same depth as for the samples damaged at 295 K. Due to defect evolution at 800 K the number of traps is reduced and hence the deuterium concentration found in this sample is substantially lower. The maximum deuterium concentration is 0.55 at-% and hence a factor of 3.5 smaller than for the samples damaged at 295K. The total amount of deuterium retained in the self-damaged layer is 5.4×10^{20} D/m^2. It is worth mentioning that deuterium uptake for these samples damaged at 800 K is substantially larger than observed in an independent study of the same material conducted recently [29]. There the tungsten samples self-damaged at 800 K were loaded with a beam of atomic deuterium at 600 K and a maximum concentration of 0.14 at.% was observed. Hence thermal detrapping between D loading at 295 K and at 600 K reduces D retention by a factor of four for this type of self-damaged material.

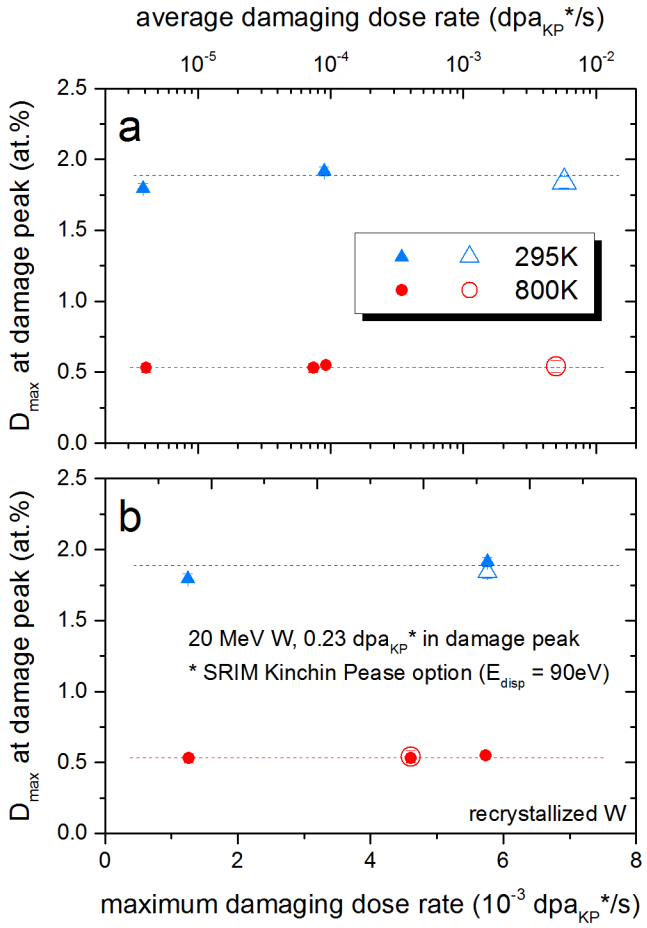

Figure 5: Maximum deuterium concentration in the self-damaged zone for recrystallized tungsten damaged with 20 MeV W^{6+} at 295 K and 800 K as function of a) average damaging dose rate and b) peak damage dose rate. D decoration was done for 72 h (1.45×10^{25} D/m^2) with <5 eV/D at 295 K. Closed symbols: scanned beam, open symbols: continuous beam.

Figure 5 shows the maximum concentrations of this experimental series for all samples conducted in the same way as the first one except that damaging was conducted at 800 K. Also here, variation of the damage dose rate does not influence deuterium uptake. This is rather surprising. Reduction in D retention by a factor of 3.5 clearly points towards a reduced defect density and hence defect evolution taking place between 300 K and 800 K as shown also in [29]. One could therefore expect an influence of the damage rate. Obvioulsy time scales in defect evolution are faster than defined by these damage rates.

In a recent study Gilbert et al. calculated the expected damage for DEMO to be smaller than 14 dpa per full power year which converts to a damage rate of around 4×10^{-7} dpa/sec. [30]. In a recent work by You et al. even smaller values for damage creation in DEMO are mentioned which convert to damage rates of 2×10^{-7} dpa/s [31]. Both values are at least one order of magnitude smaller than the average damage rates and more than three orders of magnitude smaller than the peak damage rate accessible in this experimental work. However, given the fact that no influence of deuterium retention is observed for these high rates one can safely assume that for even smaller damage dose rates no influence on D retention is present. Likewise one could conclude from these experiments that the use of a scanned ion beam instead of a continuous beam has no tremendous effect on deuterium retention studies as could have been anticipated from the experience on swelling.

4. Conclusions

Deuterium retention was measured in recrystallized tungsten implanted with 20 MeV tungsten ions at 295 K and 800 K for different damaging dose rates. Changing the average damaging dose rate by three orders of magnitude between 6×10^{-3} to 4×10^{-6} dpa/s or the peak damage dose rate by a factor of five does not influence D retention. Neither for the room temperature series, nor for the 800 K series, where defect evolution clearly takes place, as can be seen by the reduced deuterium uptake. Obviously, the time scales for defect evolution are short enough to happen in between single cascade events in both cases. As damaging rates by fusion neutrons in future fusion devices will be even smaller and hence timescale between events larger no effect of the lower damage rates on D

retention in a future reactor is to be expected However, as neutrons will not only create displacement damage but will also lead to transmutation and gas production care must be taken when extrapolating results from ion-beam-damaged tungsten to fission or fusion neutron damaged tungsten in general.

Acknowledgments

I thank J. Dorner, M. Fusseder, for their help with W ion implantation and Nuclear Reaction Analysis and G. Matern for polishing the samples and my colleagues at the plasma material interaction group for valuable discussions. Special thanks to K. Schmid for the patience in showing me how to use his NRADC code and adopting the code to my special requests. Stimulating discussions with S. Markelj on D uptake in self-damaged tungsten, defect annealing and NRA depth profiling are greatly acknowledged.

Part of this work has been carried out within the framework of the EUROfusion Consortium and has received funding from the Euratom research and training programme 2014-2018 under grant agreement No 633053. The views and opinions expressed herein do not necessarily reflect those of the European Commission.

References

[1] M. Shimada, G. Cao, T. Otsuka, M. Hara, M. Kobayashi, Y. Oya, and Y. Hatano. "Irradiation Effect on Deuterium Behaviour in Low-Dose HFIR Neutron-Irradiated Tungsten." Nuclear Fusion 55, no. 1 (2015): 13008. doi:10.1088/0029-5515/55/1/013008.

[2] G.S.Was, Fundamentals of Radiation Material Science: Metals and Alloys, Springer Berlin (2010), ISBN 978-3-540-49472-0 (2010).

[3] G.M. Wright, D.G. Whyte, B. Lipschultz. "Measurement of hydrogenic retention and release in molybdenum with the DIONISOS experiment", J. Nucl. Mater. 390–391 (2009) 544–549.

[4] W.R. Wampler and R.P. Doerner, "The influence of displacement damage on deuterium retention in tungsten exposed to plasma", Nucl. Fusion 49, 2009) 115023, doi:10.1088/0029-5515/49/11/115023.

[5] B. Tyburska, V.Kh. Alimov, O.V. Ogorodnikova, K. Schmid, and K. Ertl. "Deuterium Retention in Self-Damaged Tungsten." Journal of Nuclear Materials 395, no. 1–3 (2009): 150–55. doi:10.1016/j.jnucmat.2009.10.046.

[6] A. Založnik, S. Markelj, T. Schwarz-Selinger, Ł. Ciupiński, J. Grzonka, P. Vavpetič, and P. Pelicon. "The Influence of the Annealing Temperature on Deuterium Retention in Self-Damaged Tungsten." Physica Scripta T167 (2016): 14031. doi:10.1088/0031-8949/T167/1/014031.

[7] S. Markelj, A. Založnik, T. Schwarz-Selinger, O.V. Ogorodnikova, P. Vavpetič, P. Pelicon, and I. Čadež:.In Situ NRA Study of Hydrogen Isotope Exchange in Self-Ion Damaged Tungsten Exposed to Neutral Atoms., Journal of Nuclear Materials 469 (2016): 133–44. doi:10.1016/j.jnucmat.2015.11.039.

[8] PLANSEE Metall GmbH - High Performance Materials, A-6600 Reutte, Austria. http:// www.plansee.com.

[9] A. Manhard, Deuterium Inventory in Tungsten after Plasma Exposure: A Microstructural Survey, Ph.D. Thesis, University Augsburg, 2012.

[10] A. Manhard, G. Matern, M. Balden: A step-by-step analysis of the polishing process for tungsten specimens, Pract. Metallogr. 50(1) , 6-15 (2013).

[11] A. Manhard, M. Balden, S. Elgeti: Quantitative microstructure and defect density analysis of polycrystalline tungsten reference samples after different heat treatments, Pract. Metallorg. 52 (2015) 437.

[12] A. Manhard, S. Kapser, L. Gao, M. Balden, S. Elgeti, T. Schwarz-Selinger, U. von Toussaint, T. Płociński, J. Grzonka, M. Gloc, Ł. Ciupiński "Microstructure and Defect Analysis in the Vicinity of Blisters in Polycrystalline Tungsten", these proceeding.
[13] J. Roth, T. Schwarz-Selinger, V.Kh. Alimov, and E. Markina. "Hydrogen Isotope Exchange in Tungsten: Discussion as Removal Method for Tritium." Journal of Nuclear Materials 432, no. 1–3 (2013): 341–47. doi:10.1016/j.jnucmat.2012.08.004.
[14] E. Markina, M. Mayer, A. Manhard, and T. Schwarz-Selinger. "Recovery Temperatures of Defects in Tungsten Created by Self-Implantation." Journal of Nuclear Materials 463 (2015): 329–32. doi:10.1016/j.jnucmat.2014.12.005.
[15] T. Schwarz-Selinger, W. Jacob: Deuterium Retention in self-damaged tungsten: Saturation effects, in preparation.
[16] M. Mayer, SIMNRA User's Guide, Report IPP 9/113, Max-Planck-Instutut für Plasmaphysik, Garching, Germany, 1997 and http://www.rzg.mpg.de/~mam/
[17] J.F. Ziegler, www.srim.org.
[18] O.V. Ogorodnikova, B. Tyburska, V. Kh. Alimov, and K. Ertl. "The Influence of Radiation Damage on the Plasma-Induced Deuterium Retention in Self-Implanted Tungsten." Journal of Nuclear Materials, Proceedings of the 19th International Conference on Plasma-Surface Interactions in Controlled Fusion, 415, no. 1, Supplement (2011): S661–66. doi:10.1016/j.jnucmat.2010.12.012.
[19] R.E. Stoller, M. B. Toloczko, G. S. Was, A. G. Certain, S. Dwaraknath, and F. A. Garner. "On the Use of SRIM for Computing Radiation Damage Exposure." Nuclear Instruments and Methods in Physics Research Section B: Beam Interactions with Materials and Atoms 310 (2013): 75–80. doi:10.1016/j.nimb.2013.05.008.
[20] K. Nordlund, A.E. Sand, F. Granberg, S.J. Zinkle, R.E. Stoller, R.S. Averback, T. Suzudo, L. Malerba, F. Banhart, W.J. Weber,F. Willaime, S. Dudarev, D. Simeone, "Primary Radiation Damage in Materials", Report prepared by the OECD/NEA Working Party on Multiscale Modelling of Fuels and Structural Materials for Nuclear Systems, Expert Group on Primary Radiation Damage Nuclear Science NEA/NSC/DOC(2015)9; www.oecd-nea.org
[21] ASTM Int'l E521-96 Standard Practice for Neutron Radiation Damage Simulation by Charge-Particle Irradiation, Annual Book of ASTM Standards vol 12.02 (Philadelphia, PA: American Society for Testing and Materials) p 7 DOI
[22] A. Manhard, T. Schwarz-Selinger, W. Jacob: Quantification of the deuterium ion fluxes from a plasma source, Plasma Sources Sci. Technol. 20 (2011) 015010.
<u>Note</u>: Unfortunately, the information given in the last paragraph of this article is not correct. The contribution of the molecular ions to the total ion flux for standard conditions is: D_3^+ = 94%, D_2^+ = 3%, and D^+ = 3%. Correspondingly, the contributions to the total deuteron flux in form of ions are: 97%, 2%, and 1% as expressed correctly in figures 5 and 6 in this reference.
[23] K. Schmid and U. von Toussaint: Statistically sound evaluation of trace element depth profiles by ion beam analysis, Nucl. Instr. and Meth. in Phys. Res. B 281 64 (2012).
[24] M. Mayer: "RESOLNRA: A New Program for Optimizing the Achievable Depth Resolution of Ion Beam Analysis Methods." Nuclear Instruments and Methods in Physics Research Section B: Beam Interactions with Materials and Atoms 266, no. 8 (2008): 1852–57. doi:10.1016/j.nimb.2007.11.071.
[25] B. Wielunska, M. Mayer, T. Schwarz-Selinger, U. von Toussaint, J. Bauer: Cross section data for the D(3He,p)4He nuclear reaction from 0.25 to 6 MeV, Nucl. Instr. Meth. 371, 41-45 (2016).
[26] W. Möller and F. Besenbacher: A note on the ^{3}He+D nuclear reaction cross section, Nucl. Instr. Meth. 168, (1980), 111.
[27] T. Ahlgren, K. Heinola, K. Vörtler, and J. Keinonen. "Simulation of Irradiation Induced Deuterium Trapping in Tungsten." Journal of Nuclear Materials 427, no. 1–3 (2012): 152–61. doi:10.1016/j.jnucmat.2012.04.031.
[28] L.K. Keys and J. Moteff, Neutron Irradiation and Defect Recovery of Tungsten, J. Nucl. Mater. 34 (1970), 260-280.

[29] S. Markelj, T. Schwarz-Selinger, A. Založnik, M. Kelemen, P. Vavpetič, P. Pelicon, E. Hodille, C Grisolia: The first study of deuterium retention in tungsten simultaneously damaged by high energy W ions and loaded by D atoms, http://dx.doi.org/10.1016/j.nme.2016.11.010 in press.

[30] M.R. Gilbert,, S. L. Dudarev, D. Nguyen-Manh, S. Zheng, L. W. Packer, and J. -Ch. Sublet. "Neutron-Induced Dpa, Transmutations, Gas Production, and Helium Embrittlement of Fusion Materials." Journal of Nuclear Materials, 442, no. 1–3, Supplement 1 (November 2013): S755–60. doi:10.1016/j.jnucmat.2013.03.085.

[31] J.H. You, E. Visca ,Ch. Bachmann ,T. Barrett , F. Crescenzi, M. Fursdon, H. Greuner, D. Guilhem, P. Languille, M. Li, S. McIntosh, A.von Müller, J. Reiser, M. Richou, M. Rieth: „European DEMO divertor target: Operational requirements and material-design interface", Nuclear Materials and Energy in press (2016).